

ОБЪЕДИНЕННЫЙ  
ИНСТИТУТ  
ЯДЕРНЫХ  
ИССЛЕДОВАНИЙ  
ДУБНА

3538/82

2/viii-82  
E1-82-377

**A STUDY  
OF THE PROTON MOMENTUM SPECTRUM  
FROM DEUTERON FRAGMENTATION  
AT 8.9 GeV/c  
AND AN ESTIMATE  
OF ADMIXTURE PARAMETERS  
FOR THE SIX-QUARK STATE IN DEUTERON\***

Submitted to "Nuclear Physics B"

\* Dedicated to V.I. Veksler on his 75th birthday.

**1982**

V.G.Ableev<sup>1</sup>, D.A.Abdushukurov<sup>2</sup>, S.A.Avramenko,  
Ch.Dimitrov<sup>3</sup>, A.Filipkowski<sup>4</sup>, A.P.Kobushkin<sup>5</sup>,  
D.K.Nikitin<sup>2</sup>, A.A.Nomofilov, N.M.Piskunov, V.I.Sharov,  
I.M.Sitnik, E.A.Strokovsky, L.N.Strunov, L.Vizireva<sup>6</sup>,  
G.G.Vorobiev, S.A.Zaporozhets

Scientific Construction Device, Bulgarian  
Academy of Sciences, Sofia, Bulgaria.

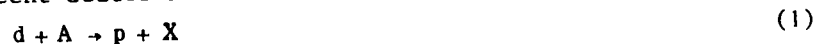
<sup>4</sup>Institute for Nuclear Research, Warsaw,  
Poland.

<sup>5</sup>Institute for Theoretical Physics,  
Ukrainian SSR Academy of Sciences, Kiev,  
USSR.

<sup>6</sup>High Chemical-Technological Institute,  
Sofia, Bulgaria.

## INTRODUCTION

Many authors<sup>/1/</sup> have pointed to the importance of obtaining data on the high momentum distribution of nucleons in deuteron for understanding its short-range structure and verifying recent deuteron models. The stripping reaction



is, in particular, a source of such information on the deuteron wave function (DWF). Experimental data on the reaction (1) can be used to estimate parameters of the hybrid model<sup>/2,3/</sup> in which the DWF is a superposition of two weakly bound three-quark ( $np$ -state) and of six-quark ( $6q$ -state) clusters. Indeed, the calculation<sup>/4/</sup> by this model shows that the differential cross section of the reaction (1) is sensitive to the contribution of the  $6q$ -state in the region of proton longitudinal momenta  $p_{\parallel}^* > 200$  MeV/c calculated in the deuteron rest frame.

To select the contribution to the spectrum from different mechanisms (Fermi motion of nucleons in the nucleus,  $6q$ -system fragmentation and so on), it is desirable to have data covering the whole kinematical region. The existing data are not sufficiently detailed. They are concentrated either in the cumulative region<sup>/5/</sup> ( $p_{\parallel}^* > 250$  MeV/c) or in the complementary region<sup>/6/</sup> ( $p_{\parallel}^* < 300$  MeV/c) and obtained from different targets.

In this paper the reaction (1) was investigated on  $^{12}\text{C}$  nuclei target at forward emission angles ( $\theta_p \leq 0.4^\circ$ ) and at a deuteron momentum of  $p_d = 8.9$  GeV/c. The proton momentum spectrum is measured in steps of 0.09 GeV/c in the region  $3.65 \leq p \leq 8.05$  GeV/c ( $-206 \leq p_{\parallel}^* \leq 580$  MeV/c). Preliminary results are presented elsewhere<sup>/7/</sup>.

The experimental procedure and data processing are described in section 2. The calculations of the spectrum by the DWF of the hybrid model are presented in section 3. Their comparison with the experiment is presented in section 4.

## 2. EXPERIMENTAL PROCEDURE AND DATA PROCESSING

The experiment has been performed in the extracted deuteron beam of the Dubna synchrophasotron. The experimental setup<sup>/8/</sup>

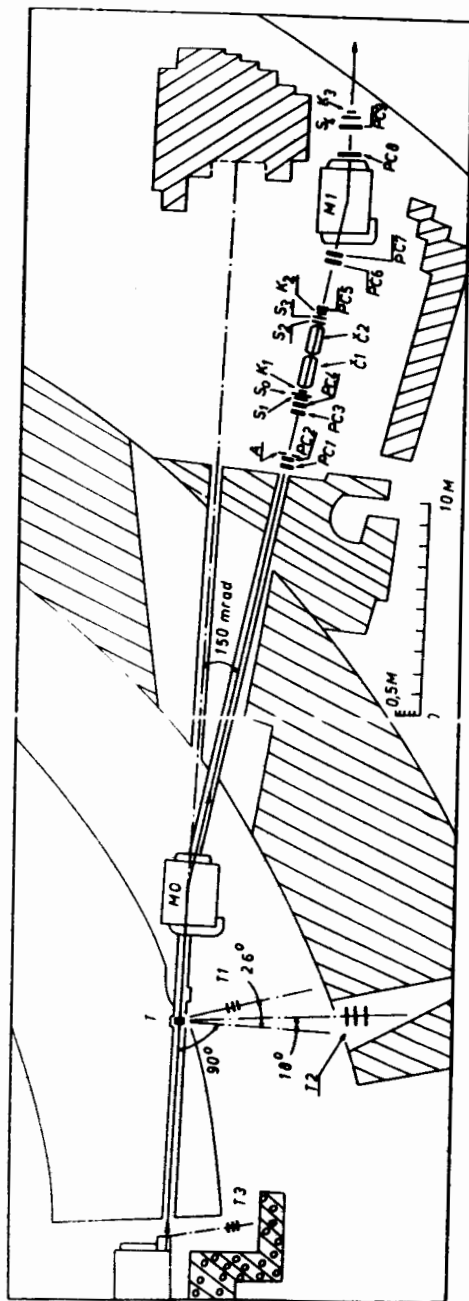


Fig. 1. Schematic layout of the experimental apparatus.

(Fig. 1) included a carbon target T (30x140x21 mm<sup>3</sup>; 3.2 g/cm<sup>2</sup>) placed in a vacuum pipe, bending (M0) and analysing (M1) magnets, scintillation (A, K<sub>1</sub>, S<sub>1</sub>, T<sub>1</sub>) and threshold Cherenkov (C<sub>1</sub>, C<sub>2</sub>) counters and multiwire proportional chambers (PCi). The detectors and readout electronics of the spectrometer<sup>9/</sup> were used on-line with an ES1010 computer.

The particles emitted from the target in the forward direction were bent by 150 mrad relative to the deuteron beam axis. The angular acceptance of the setup was determined by the S<sub>1</sub>, S<sub>2</sub>, S<sub>3</sub> (50x50 mm<sup>2</sup>) counters. The average momentum of the secondary particles was changed in steps of 0.02 p<sub>d</sub> by appropriate changing of the M0 magnetic field. To ensure the constancy of the setup relative momentum acceptance, the M1 field was changed in proportion to the M0 field so that the particles, moving along the setup axis, hit the centre of the S<sub>4</sub> counter (200x350 mm<sup>2</sup>). The magnetic field values were measured by Hall probes with a 0.1% accuracy.

A strong momentum dependence of the fragments yield demanded a variation of the deuteron intensity during data taking. The beam intensity varied over a range of 5·10<sup>8</sup> ÷ 2·10<sup>10</sup> particles/pulse so that the detector rates remained at an acceptable level of (0.5 ÷ 1.0)·10<sup>6</sup> particles/sec. The scintillation monitors T1, T2 and T3 were used for a relative measurement of the deuteron flux. Parameters of the extracted beam are controlled by interconnecting computers of the setup and the accelerator.

Data were taken with three triggers (TR1, 2, 3) interchanging "target-full" and "target-empty" runs. In the 3.5 ÷ 6.0 GeV/c momentum region data were taken mainly with TR1 = S<sub>1</sub> ^ S<sub>2</sub> ^ S<sub>3</sub> ^ S<sub>4</sub> trigger. Due to the background reaction



the deuteron component is contributed to the secondary beam at momenta higher than 6 GeV/c. In this region protons were selected by the trigger TR2 = TR1 ^ C<sub>1</sub> ^ C<sub>2</sub>, where the threshold Cherenkov counters C<sub>1</sub>, C<sub>2</sub> were tuned to detect protons with the full efficiency (99%) at momenta higher than 6 GeV/c. The trigger TR3 = K<sub>1</sub> ^ K<sub>2</sub> ^ K<sub>3</sub> ^ S<sub>0</sub> ^ A<sup>-</sup> was used to check the efficiencies of the detectors.

In data processing, the particle momentum was determined by coordinate information from PC5 ÷ PC9 with an accuracy of σ<sub>p</sub>/p = 0.4%. Using both the information from PC1 ÷ PC4 and the momentum analysis, the particle trajectories were extrapolated to the target region. Both the X, Y coordinates

of the interaction point in the target (in the plane perpendicular to the deuteron beam axis) and the angle of the emitted particle (relative to the primary beam axis) were determined with accuracies of  $\sigma_{x,y} = 10$  mm and  $\sigma_\theta = 0.8$  mrad, respectively. Events originating from the matter surrounding the target were rejected by appropriate cuts in the X, Y coordinates. The restriction on momentum was also introduced. Events were selected from an interval of  $P_0 \cdot (1+0.06)$ , where  $P_0$  is the momentum of the particle moving parallel to the setup axis. The size of the momentum interval was determined by the condition that the corrections for geometric efficiency at its boundaries were no more than 30%. For this interval the emission angles accepted by the setup were located in the region  $|\theta_x - \theta_0| \leq 2$  mrad and  $|\theta_y| \leq 2$  mrad. The  $\theta_0$  value was proportional to the particle momentum and varied between (-7; 7) mrad.

The deuteron contamination of the secondary beam has been taken into account. The efficiency of the Cherenkov counters,  $\epsilon_d$ , for the deuterons from reaction (2) was determined for the momenta above 8.1 GeV/c kinematically forbidden for protons:  $\epsilon_d = (1.04 \pm 0.12) \times 10^{-3}$ . This value, along with the values of the reaction (2) differential cross sections measured in the trigger TR1 conditions, was used to correct the proton spectrum for the deuteron admixture. The corrections were 10% at 7.5 GeV/c and 90% at 8.0 GeV/c.

Corrections due to background events determined from the "empty" target runs were about 10% for each part of the spectrum.

The absolute normalization of experimental data was performed using a calibrating measurement of the differential cross section of the studied process for proton-fragment momenta near  $p_d/2$ . In this measurement performed at the reduced deuteron beam intensity  $\sim 10^6$  particles/pulse both the arrangement of the detectors and the measuring procedure were similar to that described in ref. <sup>10</sup>.

The experimental results are presented in Table 1 and Fig. 2. The statistical errors are shown only. The systematic errors due to the normalization were estimated to be less than 3%.

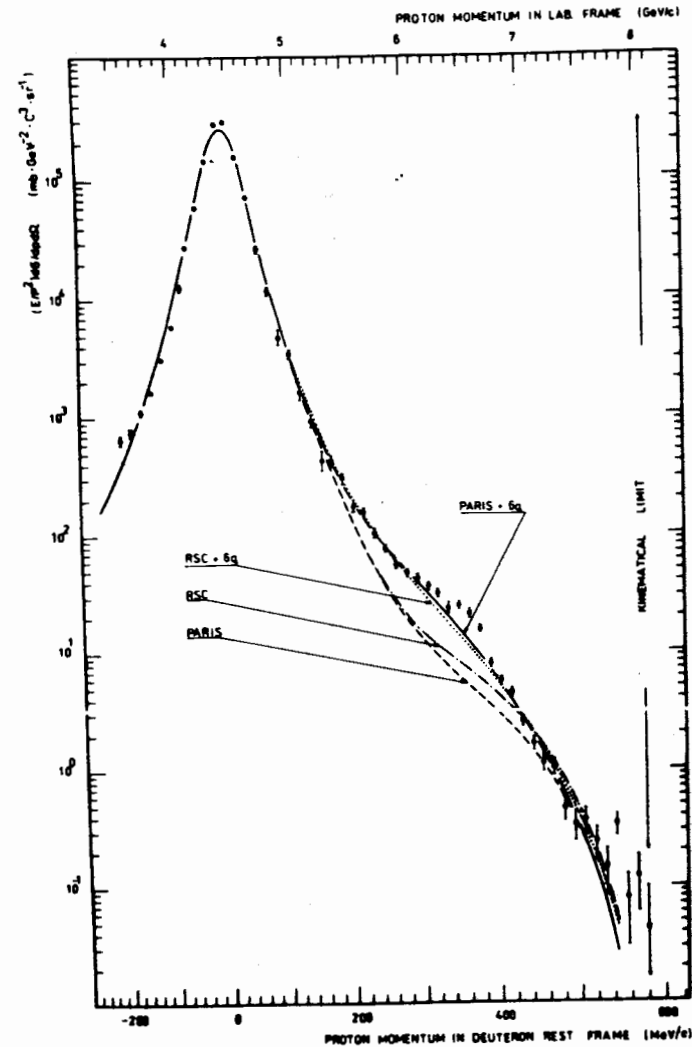


Fig. 2. Invariant cross sections for the reaction (1). The curves correspond to the hybrid model DWF calculations with two-nucleon wave function of the Paris NN potential (solid) and the Reid soft-core one (dotted). The corresponding values of the  $6q$ -admixture parameters are taken from Table 3. The dashed and dashed-dotted curves are the calculations with these wave functions but without  $6q$ -admixture.

of the interaction point in the target (in the plane perpendicular to the deuteron beam axis) and the angle of the emitted particle (relative to the primary beam axis) were determined with accuracies of  $\sigma_{x,y} = 10$  mm and  $\sigma_\theta = 0.8$  mrad, respectively. Events originating from the matter surrounding the target were rejected by appropriate cuts in the X, Y coordinates. The restriction on momentum was also introduced. Events were selected from an interval of  $P_0 \cdot (1 \pm 0.06)$ , where  $P_0$  is the momentum of the particle moving parallel to the setup axis. The size of the momentum interval was determined by the condition that the corrections for geometric efficiency at its boundaries were no more than 30%. For this interval the emission angles accepted by the setup were located in the region  $|\theta_x - \theta_0| \leq 2$  mrad and  $|\theta_y| \leq 2$  mrad. The  $\theta_0$  value was proportional to the particle momentum and varied between (-7; 7) mrad.

The deuteron contamination of the secondary beam has been taken into account. The efficiency of the Cherenkov counters,  $\epsilon_d$ , for the deuterons from reaction (2) was determined for the momenta above 8.1 GeV/c kinematically forbidden for protons:  $\epsilon_d = (1.04 \pm 0.12) \times 10^{-3}$ . This value, along with the values of the reaction (2) differential cross sections measured in the trigger TR1 conditions, was used to correct the proton spectrum for the deuteron admixture. The corrections were 10% at 7.5 GeV/c and 90% at 8.0 GeV/c.

Corrections due to background events determined from the "empty" target runs were about 10% for each part of the spectrum.

The absolute normalization of experimental data was performed using a calibrating measurement of the differential cross section of the studied process for proton-fragment momenta near  $p_d/2$ . In this measurement performed at the reduced deuteron beam intensity  $\sim 10^6$  particles/pulse both the arrangement of the detectors and the measuring procedure were similar to that described in ref. /10/.

The experimental results are presented in Table 1 and Fig. 2. The statistical errors are shown only. The systematic errors due to the normalization were estimated to be less than 3%.

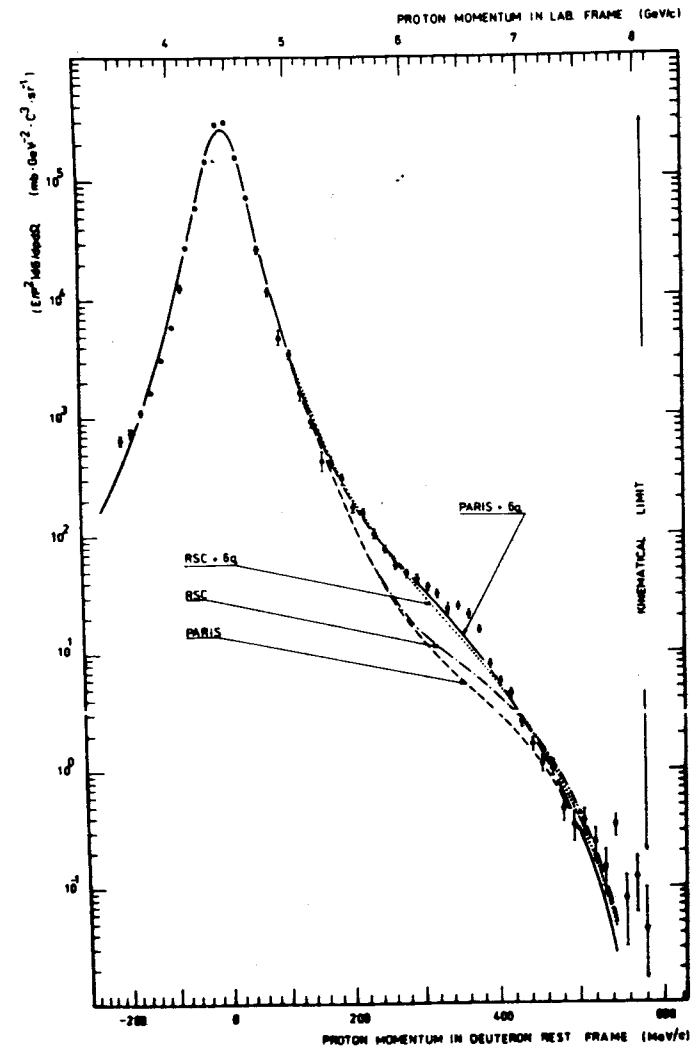


Fig. 2. Invariant cross sections for the reaction (1). The curves correspond to the hybrid model DWF calculations with two-nucleon wave function of the Paris NN potential (solid) and the Reid soft-core one (dotted). The corresponding values of the  $6q$ -admixture parameters are taken from Table 3. The dashed and dashed-dott curves are the calculations with these wave functions but without  $6q$ -admixture.

Table 1

Momentum spectrum of protons emitted at small angles in the stripping reaction  $d+C \rightarrow p+X$  at a deuteron momentum of 8.9 GeV/c

NN	Proton momentum in the laboratory frame p (GeV/c)	Invariant cross section $(E/p^2) d\sigma/dp d\Omega$ mb GeV <sup>-2</sup> c <sup>3</sup> sr <sup>-1</sup>	Proton momentum in the deuteron rest frame p <sub>  </sub> <sup>*</sup> (MeV/c)
1	2	3	4
1	3.56	$(6.45 \pm 0.58) \times 10^2$	- 206
2	3.65	$(7.36 \pm 0.62) \times 10^2$	- 183
3	3.74	$(1.10 \pm 0.05) \times 10^3$	- 160
4	3.83	$(1.62 \pm 0.06) \times 10^3$	- 138
5	3.92	$(3.06 \pm 0.11) \times 10^3$	- 117
6	4.01	$(5.86 \pm 0.16) \times 10^3$	- 96
7	4.09	$(1.23 \pm 0.06) \times 10^4$	- 78
8	4.14	$(2.72 \pm 0.14) \times 10^4$	- 67
9	4.23	$(5.87 \pm 0.19) \times 10^4$	- 47
10	4.32	$(1.42 \pm 0.05) \times 10^5$	- 28
11	4.41	$(2.83 \pm 0.08) \times 10^5$	- 9
12	4.49	$(2.96 \pm 0.10) \times 10^5$	8
13	4.58	$(1.54 \pm 0.05) \times 10^5$	26
14	4.67	$(7.14 \pm 0.28) \times 10^4$	44
15	4.76	$(2.60 \pm 0.16) \times 10^4$	61
16	4.85	$(1.14 \pm 0.09) \times 10^4$	79
17	4.94	$(4.66 \pm 0.63) \times 10^3$	96
18	5.03	$(3.38 \pm 0.29) \times 10^3$	113
19	5.12	$(1.60 \pm 0.23) \times 10^3$	129
20	5.21	$(9.11 \pm 1.07) \times 10^2$	145
21	5.30	$(4.22 \pm 0.77) \times 10^2$	161
22	5.38	$(4.17 \pm 0.41) \times 10^2$	175
23	5.47	$(2.95 \pm 0.33) \times 10^2$	191
24	5.56	$(1.73 \pm 0.19) \times 10^2$	206
25	5.65	$(1.52 \pm 0.11) \times 10^2$	222
26	5.74	$(1.01 \pm 0.08) \times 10^2$	237
27	5.83	$(7.58 \pm 0.43) \times 10^1$	252
28	5.92	$(5.51 \pm 0.42) \times 10^1$	266
29	6.01	$(4.66 \pm 0.33) \times 10^1$	281

1	2	3	4
30	6.10	$(4.24 \pm 0.31) \times 10^1$	295
31	6.19	$(3.59 \pm 0.27) \times 10^1$	310
32	6.27	$(3.13 \pm 0.23) \times 10^1$	322
33	6.36	$(2.35 \pm 0.24) \times 10^1$	336
34	6.45	$(2.45 \pm 0.16) \times 10^1$	350
35	6.54	$(2.09 \pm 0.17) \times 10^1$	364
36	6.63	$(1.53 \pm 0.10) \times 10^1$	378
37	6.72	$(7.86 \pm 0.59) \times 10^0$	391
38	6.81	$(5.55 \pm 0.46) \times 10^0$	404
39	6.90	$(4.40 \pm 0.38) \times 10^0$	418
40	6.99	$(2.50 \pm 0.25) \times 10^0$	431
41	7.08	$(1.62 \pm 0.21) \times 10^0$	444
42	7.16	$(1.11 \pm 0.16) \times 10^0$	456
43	7.25	$(1.01 \pm 0.14) \times 10^0$	469
44	7.34	$(4.54 \pm 0.93) \times 10^{-1}$	482
45	7.43	$(3.30 \pm 0.89) \times 10^{-1}$	494
46	7.52	$(3.62 \pm 0.86) \times 10^{-1}$	507
47	7.61	$(2.36 \pm 0.72) \times 10^{-1}$	520
48	7.70	$(1.44 \pm 0.59) \times 10^{-1}$	532
49	7.79	$(3.36 \pm 0.70) \times 10^{-1}$	545
50	7.88	$(7.79 \pm 4.75) \times 10^{-2}$	557
51	7.97	$(1.19 \pm 0.59) \times 10^{-1}$	569
52	8.05	$(4.27 \pm 5.48) \times 10^{-2}$	580

### 3. CALCULATION OF THE SPECTRUM WITHIN THE HYBRID MODEL OF THE DWF

The invariant cross section for the reaction(1) was calculated in the framework of the Glauber-Sitenko theory using the formula<sup>11/</sup>

$$E_p \frac{d^3\sigma}{dp^3} = C_d \frac{a_{max} - a}{(2a_{max} - 1)(1 - a)} [|\Phi(\vec{p}_\perp, a)|^2 \sigma_{NA}^T - 2 \text{Re} \Phi^*(\vec{p}_\perp, a) \int d\vec{q}_\perp \Phi(\vec{q}_\perp, a) \sigma_{NA}(\vec{q}_\perp) + \int d\vec{q}_\perp |\Phi(\vec{q}_\perp, a)|^2 \sigma_{NA}(\vec{q}_\perp)] \quad (3)$$

where  $\sigma_{NA}^T$  is the total nucleon-nucleus cross section and  $\sigma_{NA}(\vec{q}_\perp)$  the elastic nucleon-nucleus differential cross section

on for nucleus A. The coefficient  $C_d$  was introduced in order to take into account only deuteron breakup events from all processes occurring in deuteron-nucleus collisions:

$$C_d \approx \sigma_{dA}^{\text{in}} / \sigma_{dA}^{\text{T}}. \quad (4)$$

Here  $\sigma_{dA}^{\text{in}}$  is the total inelastic deuteron-nucleus cross section and  $\sigma_{dA}^{\text{T}}$  the total deuteron-nucleus cross section. For the

carbon nuclei  $\sigma_{NA}^{\text{T}}=380$  mb,  $\sigma_{NA}(\vec{q}_\perp) = \frac{A}{\pi} \exp(-Bq_\perp^2)$ ,  
 $A=7500$  mb  $(\text{GeV}/c)^{-2}$ ,  $B=65$   $(\text{GeV}/c)^{-2}$  and  $C_d=0.54$ .

As a relativistic DWF in (3), we have used the wave function  $\Phi(\vec{p}_\perp, a)$  in terms of the light cone variables<sup>/13/</sup>  $\vec{p}_\perp$  and  $a = \frac{E_p + p_{\parallel}}{E_d + p_{\parallel}}$ . The advantages of such DWF relativization are pointed out in refs.<sup>/14,15/</sup>. In particular, at high deuteron energies, off-mass shell effects become unimportant, and the relativistic DWF is simply related to the nonrelativistic one  $\phi_{\text{nonrel}}$  by the expression:

$$|\Phi(\vec{p}_\perp, a)|^2 = \frac{1}{4(1-a)} \sqrt{\frac{m^2 + p_\perp^2}{a(1-a)}} |\phi_{\text{nonrel}}(\frac{m^2 + p_\perp^2}{4a(1-a)} - m^2)|^2. \quad (5)$$

The DWF (5) takes into account the boundaries of phase space volume for infinite deuteron momentum. Therefore; at finite deuteron momentum, the factor  $(a_{\text{max}} - a) / [(2a_{\text{max}} - 1)(1 - a)]$  was introduced into (3).

In the hybrid model of the DWF with the oscillator potential of interquark interaction, the nonrelativistic  $\phi_{\text{nonrel}}(\vec{k}^2)$  was replaced<sup>/4/</sup> by

$$\phi_{\text{nonrel}}(\vec{k}^2) = \sqrt{1 - |\beta|^2} \phi_{\text{nonrel}}^{\text{np}}(\vec{k}^2) + \beta \phi_{\text{nonrel}}^{\text{Bq}}(\vec{k}^2), \quad (6)$$

where

$$\phi_{\text{Bq}}(\vec{k}^2) = I \cdot \sqrt{20} (2 / (1 + \sqrt{2}))^6 \cdot 2^{3/2} \left( \frac{2}{3\pi\omega} \right)^{3/4} \exp(-\vec{k}^2 / (3\omega)), \quad (7)$$

$$\vec{k}_\perp = \vec{p}_\perp, \quad k_3 = (a - \frac{1}{2}) \sqrt{\frac{m^2 + p_\perp^2}{a(1-a)}}.$$

Factor  $I \approx 0.332$  is the overlap factor of color spin-isospin wave functions and  $\omega$  defines the root-mean-square radius of the  $\text{Bq}$  system  $r_{\text{Bq}}^2 = 5 / (4\omega)$ . The squared modulus  $(|\beta|^2)$  of the complex parameter  $\beta = |\beta| \exp(i\kappa)$  presents the value of  $\text{Bq}$ -admixture in deuteron, and the phase ( $\kappa$ ) takes into account the degree of nonorthogonality between the  $\text{np}$  and  $\text{Bq}$  components of the DWF. As  $\phi_{\text{nonrel}}^{\text{np}}$  we have used the wave function for the Reid soft-core potential<sup>/17/</sup> (RSC) and the

wave function for the Paris NN potential<sup>/18/</sup> (PARIS). The contribution of six-quark admixture (7) to the hybrid DWF (6) become comparable to the contribution from the  $\phi_{\text{nonrel}}^{\text{np}}$  only for large values of momentum  $\vec{k}$ .

#### 4. RESULTS AND DISCUSSION

The invariant cross sections for the reaction (1) at  $p_{\parallel}^* = 0$ , obtained in the calibrating measurement and calculated by formula (3) using the DWF<sup>/16-18/</sup>, are presented in Table 2. One can see that our calculations are practically independent

Table 2

Invariant cross sections ( $\text{b GeV}^{-2} \text{ c}^3 \text{ sr}^{-1}$ ) for the studied reaction at maximum proton yield ( $p_{\parallel}^* = 0$ )

Calibrating measurement		(281±9)
	McGee <sup>/16/</sup>	281.4
Calculation using DWF	RSC <sup>/17/</sup>	285.4
	PARIS <sup>/18/</sup>	291.2

of the DWF choice and agree with the result of the calibrating measurement. It is necessary to note that the calculation by the model<sup>/12/</sup> exceeds by 30% both the cross section measured by us and at Berkeley<sup>/12/</sup>.

The experimental spectrum was compared with the calculation in a momentum region of  $8 \leq p_{\parallel}^* \leq 580$  MeV/c (Fig.2). The cross sections calculated by the model were corrected taking into account the finite momentum resolution of the apparatus and the histogram bin size. The difference of the initial cross section from the corrected one is varied from ~10% in the maximum proton yield region to less than 1% for  $p_{\parallel}^* > 300$  MeV/c.

The normalization factor between the experimental and calculated spectrum was determined from the fit in the region  $8 \leq p_{\parallel}^* \leq 161$  MeV/c using the Reid DWF as  $\phi_{\text{nonrel}}(\vec{k}^2)$ . This factor remains constant within a 1.5% error when the region of the fit is reduced to  $8 \leq p_{\parallel}^* \leq 79$  MeV/c.

The  $6q$ -admixture parameters  $|\beta|$ ,  $\kappa$  and  $\omega$  were found from the fit in the region  $26 \leq p_{\parallel}^* \leq 580$  MeV/c using as  $\phi_{np}^{\text{nonrel}}$  both the RSC and the PARIS wave function. The two parts of the spectrum  $295 \leq p_{\parallel}^* \leq 378$  MeV/c and  $p_{\parallel}^* = 545 \pm 12$  MeV/c are excluded from the fit. The first part corresponds to the production of dibaryon resonances<sup>/23/</sup> and the  $N\Delta$  system in an intermediate state. The second one corresponds to proton knock-out from the carbon nucleus in the backward scattering process  $dp \rightarrow p(np)$ . These processes are not taken into account by our model. The values of the parameters obtained from the fit are given in Table 3. Figure 2 shows the comparison of the experiment and the calculations from which one can see that the experimental data are not described by the models without  $6q$ -admixture. A satisfactory description of the data was obtained only with the hybrid DWF. The data are

Table 3

Hybrid model parameters determined from the fit of the experimental data by theoretical formula (3) using the different DWF.  $N=28$  is the number of degrees of freedom. The errors are statistical only

DWF	Parameters of the hybrid model			
	$ \beta ^2$	$r_{6q}$ (fm)	$\kappa$ (degrees)	$\chi^2/N$
RSC	0	-	-	12.7
RSC+6q	$0.031 \pm 0.002$	$0.87 \pm 0.10$	$61 \pm 11$	2.54
PARIS	0	-	-	15.7
PARIS+6q	$0.043 \pm 0.004$	$0.95 \pm 0.05$	$82 \pm 6$	1.95

not very sensitive to choosing either RSC or PARIS two-nucleon wave functions. The parameters of  $6q$ -admixture are rather similar in both cases. The value of  $r_{6q}$  obtained from the fit agrees with its estimations in refs.<sup>/19,20/</sup>. More detailed information on the estimations of  $6q$ -admixture parameters see in refs.<sup>/21-23/</sup>.

Figure 3 shows the difference of the experimental results and calculations by the (PARIS+6q) DWF model in the region  $295 \leq p_{\parallel}^* \leq 378$  MeV/c excluded from the fit. An enhancement seen in this region could be due to the forward production of dibaryon resonance in the process

PROTON MOMENTUM IN DEUTERON REST FRAME (MeV/c)

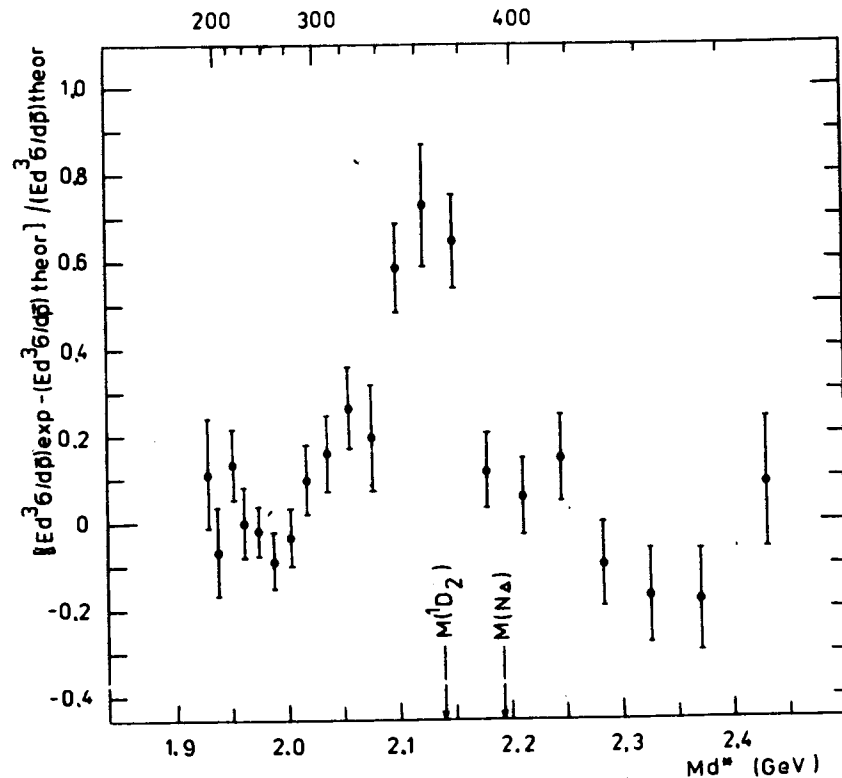
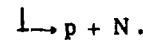


Fig.3. The proton momentum spectrum in the region  $295 \leq p_{\parallel}^* \leq 378$  MeV/c excluded from the fit.



(8)

The positions of the nearest dibaryon resonance  ${}^1D_2$  (2140),  $\Gamma \approx 80$  MeV, found in the experiment<sup>/24/</sup>, and the contribution of the  $(N\Delta)$  system in an intermediate state are marked in Fig.3 by arrows.

## 5. CONCLUSION

The proton momentum spectrum for stripping  $d + {}^{12}\text{C} \rightarrow p + X$  reaction at a deuteron momentum of 8.9 GeV/c and small emission angles has been measured in detail. The obtained data are described in the framework of the relativistic Glauber-

The  $6q$ -admixture parameters  $|\beta|$ ,  $\kappa$  and  $\omega$  were found from the fit in the region  $26 \leq p_{\parallel}^* \leq 580$  MeV/c using as  $\phi_{np}^{\text{nonrel}}$  both the RSC and the PARIS wave function. The two parts of the spectrum  $295 \leq p_{\parallel}^* \leq 378$  MeV/c and  $p_{\parallel}^* = 545 \pm 12$  MeV/c are excluded from the fit. The first part corresponds to the production of dibaryon resonances<sup>/23/</sup> and the  $\text{N}\Delta$  system in an intermediate state. The second one corresponds to proton knock-out from the carbon nucleus in the backward scattering process  $dp \rightarrow p(np)$ . These processes are not taken into account by our model. The values of the parameters obtained from the fit are given in Table 3. Figure 2 shows the comparison of the experiment and the calculations from which one can see that the experimental data are not described by the models without  $6q$ -admixture. A satisfactory description of the data was obtained only with the hybrid DWF. The data are

Table 3

Hybrid model parameters determined from the fit of the experimental data by theoretical formula (3) using the different DWF.  $N=28$  is the number of degrees of freedom. The errors are statistical only

DWF	Parameters of the hybrid model			
	$ \beta ^2$	$r_{6q}$ (fm)	$\kappa$ (degrees)	$\chi^2/N$
RSC	0	-	-	12.7
RSC+6q	$0.031 \pm 0.002$	$0.87 \pm 0.10$	$61 \pm 11$	2.54
PARIS	0	-	-	15.7
PARIS+6q	$0.043 \pm 0.004$	$0.95 \pm 0.05$	$82 \pm 6$	1.95

not very sensitive to choosing either RSC or PARIS two-nucleon wave functions. The parameters of  $6q$ -admixture are rather similar in both cases. The value of  $r_{6q}$  obtained from the fit agrees with its estimations in refs.<sup>/19,20/</sup>. More detailed information on the estimations of  $6q$ -admixture parameters see in refs.<sup>/21-23/</sup>.

Figure 3 shows the difference of the experimental results and calculations by the (PARIS+6q) DWF model in the region  $295 \leq p_{\parallel}^* \leq 378$  MeV/c excluded from the fit. An enhancement seen in this region could be due to the forward production of dibaryon resonance in the process

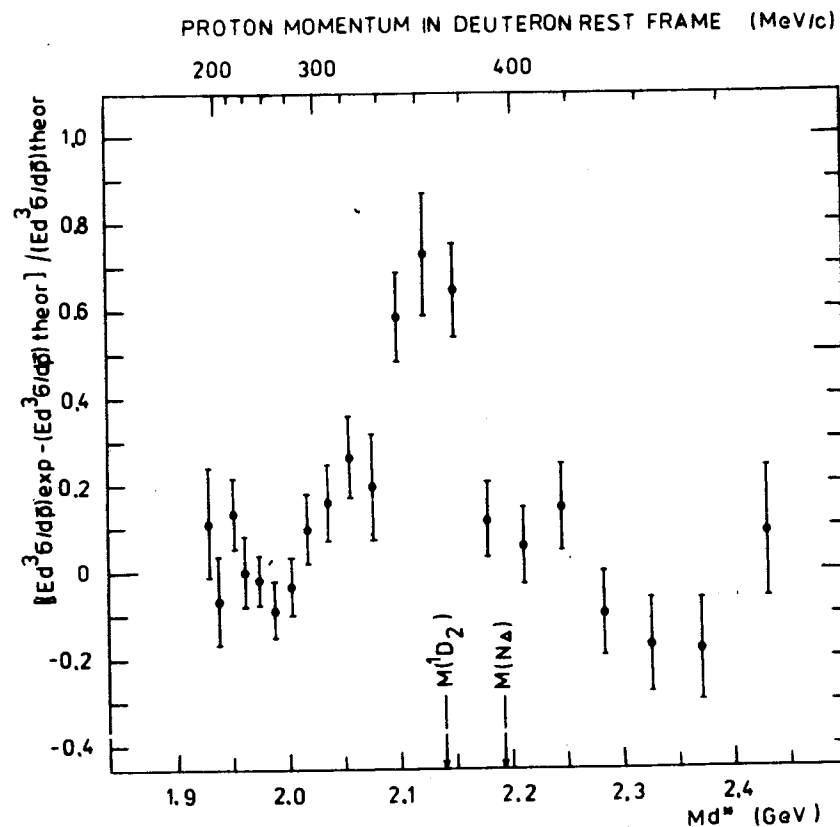
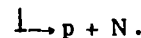


Fig.3. The proton momentum spectrum in the region  $295 \leq p_{\parallel}^* \leq 378$  MeV/c excluded from the fit.



(8)

The positions of the nearest dibaryon resonance  ${}^1D_2$  (2140),  $\Gamma \approx 80$  MeV, found in the experiment<sup>/24/</sup>, and the contribution of the  $(\text{N}\Delta)$  system in an intermediate state are marked in Fig.3 by arrows.

## 5. CONCLUSION

The proton momentum spectrum for stripping  $d + {}^{12}\text{C} \rightarrow p + X$  reaction at a deuteron momentum of 8.9 GeV/c and small emission angles has been measured in detail. The obtained data are described in the framework of the relativistic Glauber-

Sitenko theory using the hybrid deuteron wave function which includes the  $6q$ -state. The parameters of this state were estimated (see Table 3). A shoulder in the spectrum is observed in the proton momenta region  $295 \leq p_{\parallel}^* \leq 378$  MeV/c kinematically corresponding to the production of the dibaryon resonance with a mass from 2.0 to 2.2 GeV.

The authors are grateful to A.M. Baldin, V.R. Garsevanishvili, L.A. Kondratyuk, V.K. Lukyanov, V.A. Matveev, Yu.A. Simonov, L.L. Frankfurt and M.I. Strikman for fruitful discussions.

#### REFERENCES

1. Baldin A.M. Fizika Elementarnykh Chastits i Atomnogo Yadra, 1977, 8, p. 233; Prog.Part.& Nucl.Phys., 1980, 4, p. 95; Bergström L., Fredriksson S. Rev.Mod.Phys., 1980, 52, p. 675; Frankfurt L.L., Strikman M.I. Fizika Elementarnykh Chastits i Atomnogo Yadra, 1980, 11, p. 571.
2. Matveev V.A., Sorba P. Nuovo Cim.Lett., 1977, 20, p. 435.
3. Kobushkin A.P. Yad.Fiz., 1978, 28, p. 495; Preprint ITP-76-145E, Kiev, 1976.
4. Kobushkin A.P., Vizireva L. Preprint ITP-81-108E, Kiev, 1981; J.Phys.G, to be published.
5. Baldin A.M. et al. JINR, P1-11168, Dubna, 1977.
6. Papp J. LBL-3633, 1975.
7. Ableev V.G. et al. In: Abstracts of contributed papers to the 9th Int.Conf. on High Energy Physics and Nuclear Structure. Versailles, 1981, p. 70.
8. Ableev V.G. et al. JINR, 13-81-782, Dubna, 1981.
9. Ableev V.G. et al. Pribory i Tekhnika Eksperimenta, 1978, 2, p. 63.
10. Ableev V.G. et al. JINR, P1-10565, Dubna, 1977.
11. Bertocchi L., Treleani D. Nuovo Cimento, 1976, 36A, p.1.
12. Nissen-Meyer S. Nucl.Phys., 1978, A306, p. 499.
13. Dirak P.A.M. Rev.Mod.Phys., 1949, 21, p. 392.
14. Garsevanishvili V.R. et al. JINR, P2-9859, Dubna, 1976.
15. Frankfurt L.L., Strikman M.I. Yad.Fiz., 1978, 27, p. 1361; Nucl.Phys., 1979, B148, p. 107.
16. McGee I.J. Phys.Rev., 1966, 151, p. 772.
17. Alberi G., Rosa L.P., Thome Z.D. Phys.Rev.Lett., 1975, 34, p. 503C.
18. Lacombe M. et al. Phys.Rev., 1980, C21, p. 861; Phys.Lett., 1981, 101B, p. 139; Phys.Rev., 1981, C23, p. 2405.
19. Ohta S., et al. A Shell Model Study of Six Quark System, Tokyo University preprint, Tokyo 113, 1981.
20. Mulders P.J. Los Alamos National Laboratory preprint LA-UR-81-2397, Los Alamos, 1981; Phys.Rev. D, 1982, 25, No.5, p. 1269.
21. Lukyanov V.K., Titov A.I. In: Proc. of Int.Conf. on Extreme States in Nuclear Systems, Dresden, 1980, vol. 2, p. 60.
22. Simonov Yu.A. Phys.Lett., 1981, 107B, p. 1; Institute of Theoretical and Experimental Physics, preprint ITEP-142, Moscow, 1981.
23. Jaffe R.L. Phys.Rev.Lett, 1977, 38, p. 195; Mulders P.J., Aerts A.T., de Swart J.J. Phys.Rev., 1980, D21, p. 2653.
24. Auer I.P. et al. Phys.Rev.Lett., 1978, 41, p. 1436.  
See also: Hoshizaki N. Prog.Theor.Phys., 1978, 60, p. 1796. Locher M.P. SIN preprint PR-81-16, Villigen, 1981.

Received by Publishing Department  
on May 25 1982.

Аблеев В.Г. и др. Исследование импульсного спектра протонов фрагментации дейтрона при 8,9 ГэВ/с и оценка параметров примеси шестикваркового состояния в дейтроне E1-82-377

С помощью магнитного спектрометра с пропорциональными камерами и черенковскими счетчиками измерен импульсный спектр протонов с углами вылета меньше  $0,4^\circ$  из реакции стриппинга  $d + {}^{12}\text{C} \rightarrow p + X$  при импульсе дейтронов 8,9 ГэВ/с в области значений импульса протонов  $3,56 \text{ ГэВ/с} \leq p \leq 8,05 \text{ ГэВ/с}$  ( $-206 \text{ МэВ/с} \leq p_{\parallel}^* \leq 580 \text{ МэВ/с}$  в системе покоя дейтрона). Из анализа инвариантных сечений получены оценки параметров примеси шестикваркового состояния в дейтроне: величина примеси  $(3,1^{+0,2})\%$ , среднеквадратичный радиус шестикваркового состояния  $(0,87^{+0,10}) \text{ Фм}$ , относительная фаза двухнуклонной и шестикварковой компонент  $(61^\circ \pm 11^\circ)$  для двухнуклонной волновой функции Рейда с мягким кором и, соответственно,  $(4,3^{+0,4})\%$ ,  $(0,95^{+0,05}) \text{ Фм}$  и  $(82^\circ \pm 6^\circ)$  для волновой функции парижского потенциала. В области импульсов протона  $295 \text{ МэВ/с} \leq p_{\parallel}^* \leq 378 \text{ МэВ/с}$  обнаружена особенность в спектре, кинематически соответствующая рождению дибарионного резонанса с массой  $2,0 \text{ ГэВ} < M < 2,2 \text{ ГэВ}$ .

Работа выполнена в Лаборатории высоких энергий ОИЯИ.

Препринт Объединенного института ядерных исследований. Дубна 1982

Ableev V.G. et al. A Study of the Proton Momentum Spectrum from Deuteron Fragmentation at 8.9 GeV/c and an Estimate of Admixture Parameters for the Six-Quark State in Deuteron E1-82-377

The momentum spectrum of protons emitted at small angles in the stripping reaction  $d + {}^{12}\text{C} \rightarrow p + X$  has been measured at a deuteron momentum of 8.9 GeV/c. The data are described in the framework of the Glauber-Sitenko theory using the hybrid model of deuteron wave function which includes a six-quark state. The parameters of this state are determined. A shoulder in the spectrum has been observed in the proton momenta region which kinematically corresponds to the production of a dibaryon resonance with a mass from 2.0 to 2.2 GeV.

The investigation has been performed at the Laboratory of High Energies, JINR.

Preprint of the Joint Institute for Nuclear Research. Dubna 1982